In vitro corrosion testing of PVD coatings applied to a surgical grade Co–Cr–Mo alloy

J. BOLTON, X. HU
Department of Mechanical and Medical Engineering, University of Bradford, Bradford BD7 1DP, UK

Toxic effects and biological reaction of metallic corrosion and wear products are an important concern for metal on metal artificial joints. Corrosion tests were conducted to study the susceptibility to pitting and localized corrosion, with three coatings, CrN, TiN and DLC, applied to a wrought high carbon Co–Cr–Mo alloy substrate material.

Corrosion testing involved the measurement of potential time transients during immersion in a physiological solution and cyclic polarization of specimen potentials into the transpassive range followed by reversal of the potential to scan in the cathodic direction to regain the rest potential E_{rest}. Resistance to pitting and localized corrosion was assessed by determining the transpassive breakdown potential E_{bd} and if any hysteresis generated during the reverse cyclic scan may have caused crossover with the original anodic scan.

Three different surface coating conditions were tested namely: (1) as-coated, (2) polished, and (3) indented to penetrate the coating by diamond pyramid hardness indentor. Results showed that all three coatings produced significant improvements in corrosion resistance compared to performance of the wrought cobalt alloy but that some corrosive attack to both the CrN and TiN coatings occurred and some risk of attack to the cobalt alloy substrate existed due to coating defects or when damage to the coating occurred.

TiN coatings were highly effective in preventing corrosion provided they were thick enough to produce complete coverage. Thin TiN coatings displayed some tendency to encourage localized attack of the cobalt alloy at coating defects or where the coating suffered mechanical damage. CrN coatings underwent transpassive breakdown more easily and some degree of pitting at defects within the coating was observed, especially when the CrN coating was polished before the test. No corrosive attack of the cobalt alloy substrate was observed when the CrN coating was mechanically damaged by indentation.

DLC coatings produced were much thinner than either of the other two coatings and proved to be rather fragile. They were less effective in preventing apparently high corrosion currents and possibly high rates of corrosion.

Introduction

In current metal on UHMWPE polyethylene total hip arthroplasty, the generation of polyethylene wear particles at the articulating surfaces has been demonstrated to be one of the main causes of periprosthetic osteolysis and loosening in short and long term failures, [1–4]. This has led to renewed interest in metal on metal bearing system because a number of early McKee-Farrar replacements have survived for more than 20 years [5, 6]. Further studies have confirmed that the wear rate of metal implant pairings is 10 to 100 times lower than that of conventional metal on polyethylene articulations [7–9], indicating a potential to be developed into a new generation of more durable, long lifetime, hard bearing systems in total hip arthroplasty [10]. In the human body, however, implant devices are constantly exposed to living cells, tissues and biological fluids which produce a hostile environment for the survival of the implant [10]. The application of metal on metal implants may therefore introduce some other problems such as biologic reaction with metal species released from corrosion and wear. *In vitro* studies have revealed toxic effects due to cobalt chrome alloy corrosion products and wear particles, especially cobalt, and showed that intracellular corrosion is an important mechanism for the early release of cobalt ions [12]. Substantial levels of metallic products can be transferred into the host environment from implanted metallic devices [13, 14]. Cobalt concentrations in serum and chromium concentrations in both serum and urine have been found to be significantly higher in patients fitted with cobalt chromium alloy metal on metal total hip replacements than in control subjects not fitted with implants [15]. Rigorous testing and evaluation and further modification of metal on metal bearing systems must be conducted before their widespread use as total joint implants.

TABLE I Composition of high carbon wrought Co–Cr–Mo alloy

%C	%Si	%Mn	%Fe	%Cr	%Mo	%Co
0.19	< 0.1–0.2	0.7–0.8	0.41–0.43	27.1–27.3	5.7–5.8	Balance

In this study we have attempted to reduce corrosion damage that may occur with metal on metal implants by applying different hard ceramic coatings to wrought cobalt alloy substrates. The coatings used included, chromium nitride (CrN); titanium nitride (TiN) and diamond-like carbon (DLC).

Materials and methods

Relatively thick coatings were applied to a wrought high carbon grade Co–Cr–Mo alloy of the composition shown in Table I by Ion Bond (UK) Ltd. One CrN coating and two different thicknesses of TiN coatings were produced by arc evaporative physical vapor deposition (AEPVD) and the silicon metal containing hydrogenated DLC coating was produced by plasma-assisted chemical vapor deposition (PACVD). Average coating thickness measured on polished transverse sections were as follows: CrN, 8 μm: TiN, 8 and 19 μm: DLC: 4.7 μm. An uncoated high carbon (HC) Co–Cr–Mo alloy was used as the corrosion test baseline.

All samples were cut to sizes (14 × 14 mm square areas with 8 mm thick) suitable for the specimen holder using a high-speed cutting machine with care taken not to damage the coating. They were carefully cleaned with acetone before corrosion testing. Samples were mounted in a Teflon test specimen holder that was designed to expose 1 cm^2 of the specimen surface to the electrolyte via a square hole at the center of the holder. Care was taken to prevent possible leakage and crevice corrosion around the sample edges during the test. Testing was conducted in a physiological saline solution (aqueous 0.89 wt % NaCl) at room temperature, which was deaerated by bubbling dry nitrogen through the solution for 30 min before commencing each test. Specimens were immersed for 1 h before each test to allow them to reach a stable rest potential (E_{rest}). Two methods of assessing the corrosion resistance of the coatings were employed and were conducted in a three electrode corrosion cell containing the test electrode, a Calomel reference electrode and graphite auxiliary electrodes. The cell was connected to a computer-controlled scanning potentiostat.

Test method one was performed by monitoring any changes in rest potential with time when test samples exposed to the aqueous NaCl solution under open circuit conditions for 500 h. Open circuit tests were confined to the as coated condition both before and after being damaged by five 10 kg diamond pyramid hardness impressions. Only the thinner (8 μm) of the two TiN coatings was tested in this way.

The second method, cyclic polarization, utilized measurements of changes in potential produced by cyclic polarization of the anodic current above rest potential at 0.6 V/h (0.167 mV/s) to a positive potential well into any transpassive range (approximately 1400 mV above rest potential). After reaching this positive potential, the potential was scanned in the reverse cathodic direction, also at − 0.6 V/h, to assess re-passivation of the surface and any possibility that failure to re-passivate could encourage pitting corrosion.

Cyclic polarization studies were conducted on three different surface conditions for all three coatings, namely: (1) the as coated surface, (including thick and thin TiN coatings); (2) polished surface produced by diamond paste polishing for 5 min with 6 μm diamond followed by 2 min with 1 μm diamond paste; and (3) the as coated surface was also indented by 64 10 kg Vickers hardness impressions on an 8 × 8 square grid across the 10 × 10 mm corrosion area to simulate mechanical damage of the coating such as might occur by scratching, loss of adhesion, or wear. Each of these three coating conditions was ranked in terms of the potential at which transpassive breakdown first occurred (E_{bd}) and the range of potentials over which stable passive behavior was maintained ($\Delta E = E_{bd} - E_{pass}$).

After corrosion testing all corrosion surfaces were examined by scanning electron microscopy (SEM) (JEOL, JSM-6400) and optically using Normanski interference to detect surface pitting attack.

Results and discussion

Open circuit testing

As coated surface

Test results for open circuit monitoring of potential against time are shown in Fig. 1. These indicated that the uncoated cobalt alloy retained a fairly stable potential of − 250 mV throughout most of the 500 h except for periodic indications of local pitting corrosion when the potential decreased sharply before recovering rapidly back to its more stable value.

Metallographic examination confirmed that some very slight pitting attack had occurred on the polished surface of the uncoated cobalt alloy.

Materials which behave in a truly passive manner are more usually expected to show increases in electrode

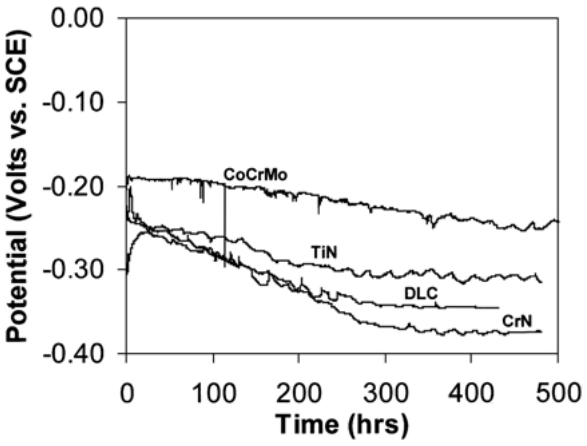

Figure 1 Open circuit potential – time transients measured on high carbon Co–Cr–Mo alloys with and without coating.

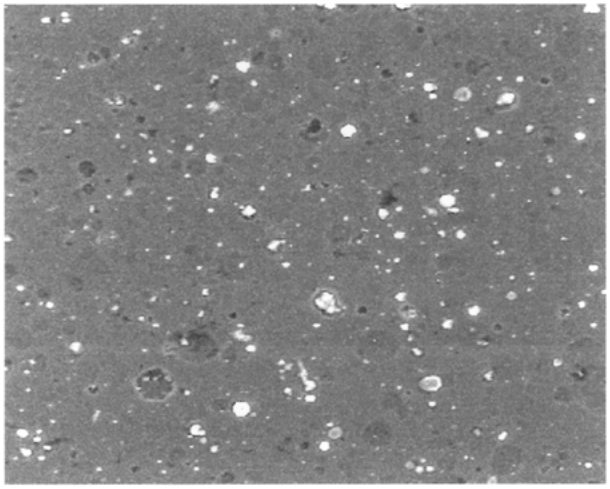

Figure 2 Slight pitting attack at defects in CrN coating after a 500 h open circuit test. SEI image. Mag × 800.

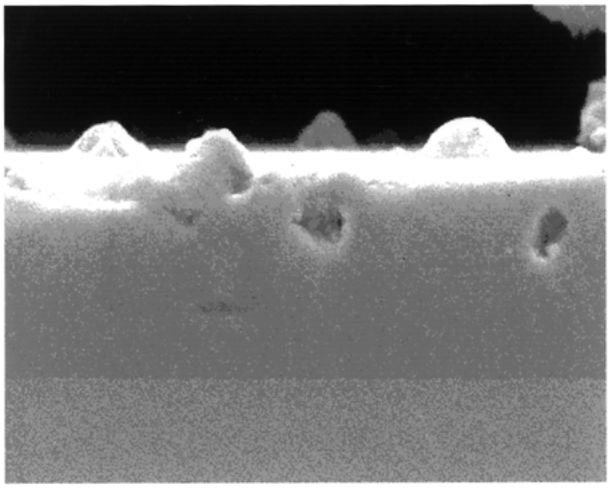

Figure 3 Possible corrosive attack at site of metal droplet in CrN coating after 500 h of open circuit exposure to aqueous saline solution. SEI image. Mag × 2700.

potential with increased times of immersion as the passive film thickens by reaction with water, any decrease in potential usually indicates some propensity for film breakdown and repair. Potentials for the coated alloys, however, showed a general trend by which the potential rose slightly in the first few hours of the test followed by fluctuating values of potential which gradually declined to reach a fairly stable level after about 300 h; final stable potentials were similar for both the as coated and indented surface and occurred at the following approximate values, CrN – 80 mV, TiN – 320 mV, DLC – 350 mV. Similar behavior where the potential declined rather than increased with time in saline solutions has also been reported for gaseously nitrided Ti-6 Al-4 V titanium alloys [16], and for sputter coated CrN coatings on an austenitic stainless steel [17]. None of the coated samples showed any sudden or sharp changes in potential such as associated with the pitting attack seen on the uncoated cobalt alloy. Examination of coated specimen surfaces after such a relatively short time as 500 h of immersion revealed little evidence of serious corrosive attack to the coating itself. Slight localized pitting attack was seen, however, at the edges of metallic micro-droplets sputtered into the structure of both the CrN and TiN coatings by the use of an arc evaporative coating technique (see Fig. 2). Such metallic micro droplets are a recognized drawback of using arc evaporative coating methods [18], and were found in both the CrN and TiN coated specimens. Significantly, the CrN coating appeared to contain more of these micro metal droplets than the TiN coating and produced the largest drop in potential.

Micro metal droplets have been shown to encourage corrosive attack in CrN coated mild steel both by attack to the droplets themselves and by providing a path through which the corrosive environment could penetrate to the substrate material. Large droplets with dimensions similar in size to the complete coating thickness and micro porosity associated with them enabled the corrosive environment to penetrate the coating and cause corrosion to take place within the mild steel substrate [19].

Defects such as micro metal droplets and their associated pores, and cracks running between metal droplets were clearly visible within the coating cross section but no penetration of the coating or consequent corrosion of the substrate cobalt alloy was seen in either the CrN or TiN coated samples, presumably because of the relatively large coating thickness used (see Fig. 3). Conclusive evidence of possible corrosive pitting attack of the metal droplets which protruded from the coating surface was not easily obtained in coatings so easily damaged by sectioning and polishing but localized pitting near to the droplets was seen more frequently in samples subjected to 500 h of open circuit corrosion testing than in samples not exposed to a corrosion test.

Indented surfaces

Little evidence of serious attack to the exposed cobalt alloy on the indented specimens was found despite the presence of potential sites for corrosive attack wherever dissimilar metal contact developed between the coating and the underlying exposed cobalt substrate and where crevices occurred at cracks formed by hardness indentation at the coating/substrate boundary. Some slight evidence of crevice attack was found at the edges of indents made in TiN and DLC coatings (see Figs 4 and 5),

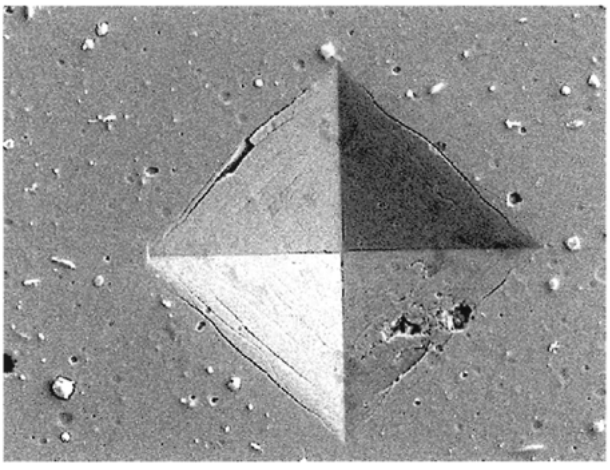

Figure 4 Slight pitting and attack of cobalt alloy substrate exposed by hardness indent made on TiN coating. Note lack of attack on the TiN surface and at cracks around the indent and within the majority of the exposed cobalt alloy. SEI image. Mag × 800.

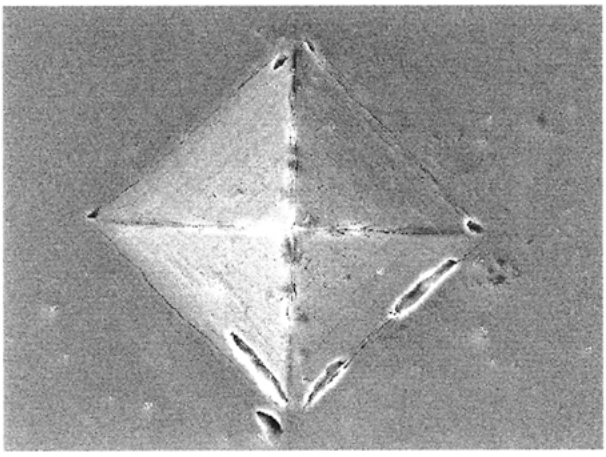

Figure 5 Slight pitting attack on the DLC coating surface and crevice attack at cracks formed at the edges of a hardness indent, after a 500 h open circuit test. SEI image. Mag × 800.

and some pitting of the cobalt substrate was found at one of the hardness indents placed in a TiN coated sample (see Fig. 4). None of the three coating types showed much tendency to cause any substantial corrosive attack of the exposed cobalt substrate.

Cyclic polarization study

Typical examples of cyclic polarization test curves for the baseline Co–Cr–Mo alloy and for each coating are shown in Fig. 6a–d. Voltage and current data used to provide information concerning the corrosion resistance of each coating type and condition are shown in Table II. These were determined from each of the cyclic polarization curves and include the following:

- rest potential E_{rest}
- breakdown potential E_{brk} and current density i_{brk} for the onset of transpassive behavior;
- passive range $\Delta E(E_{brk} - E_{\text{pass}})$
- the passivation potential E_{pass} and current i_{pass} for the start of passivation (if present) together with a pitting potential E_{pit} at the point where the reverse potential scan crossed the original anodic polarization curve (if present).

The cobalt alloy was passive at the commencement of the cyclic polarization scan but underwent serious preferential grain boundary attack by virtue of being polarized to such high potentials, well above the transpassive breakdown limit (see Fig. 7). No evidence was found to indicate the presence of either pitting or preferential attack at stringers of chromium carbide particles present in the microstructure.

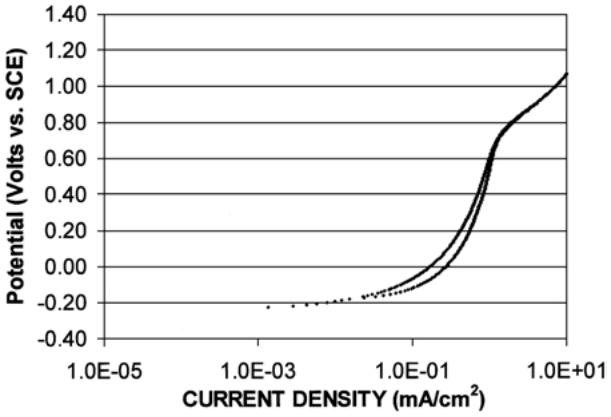

Figure 6a Cyclic polarization curve of potential versus current. CrN coating as polished.

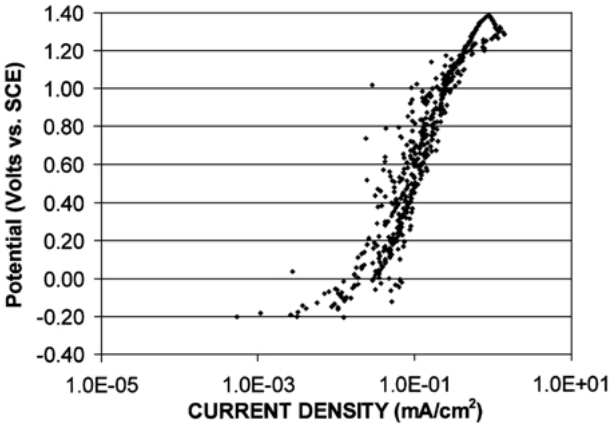

Figure 6c Cyclic polarization curve of potential versus current. Thick TiN coating, as polished.

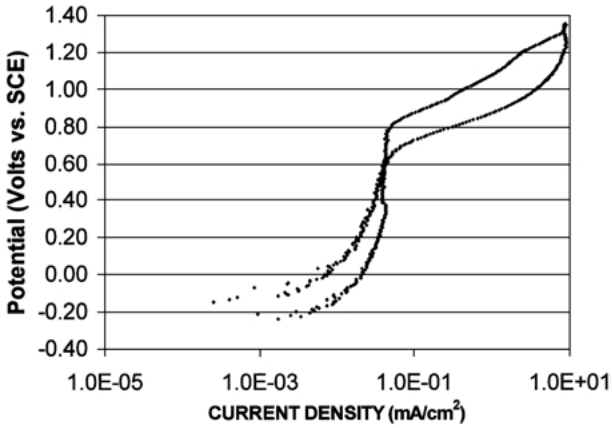

Figure 6b Cyclic polarization curve of potential versus current. Thin TiN coating indented by 10 kg hardness tests.

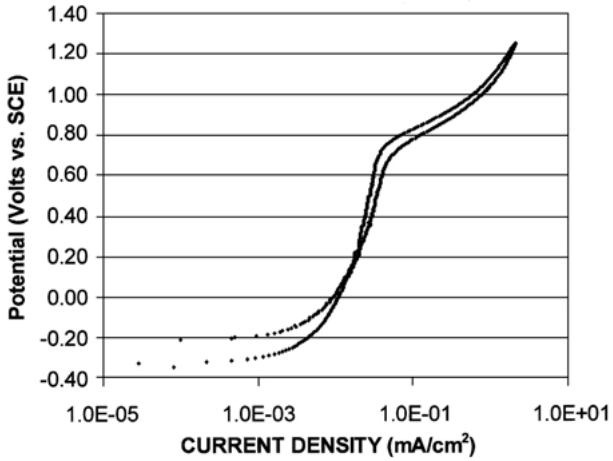

Figure 6d Cyclic polarization curve of potential versus current. DLC coating, as polished.

TABLE II Breakdown potential and currents for coated Co–Cr–Mo alloys

Alloy	E_{rest} mV	E_{brk} mV	i_{brk} mA/cm^2	ΔE mV	E_{pass} mV	i_{pass} mA/cm^2	E_{pit} mV
Uncoated Co–Cr–Mo	− 300	580	0.008	880	—		—
PVD CrN, as coated	− 200	560	0.0015	760	—		—
PVD CrN, as polished	− 230	700	1.5	900	− 200	0.15	—
PVD CrN, indented	− 200	510	0.002	710	—		—
PVD Thin TiN, as coated	− 160	980	0.06	1200	− 80	0.015	750*
PVD Thin TiN, as polished	− 200	1000	0.06	1200	− 100	0.005	800*
PVD Thin TiN, indented	− 150	800	0.07	950	0	0.015	630*
PVD Thick TiN, as coated	≈ 0	no breakdown	—	> 1600	—	—	—
PVD Thick TiN, indented	− 150	1000	0.1	1150	− 100	0.009	—
PACVD DLC, as coated	− 300	850	0.07	1130	− 180	0.002	
PACVD DLC, as polished	− 340	760	0.06	1070	− 180	0.01	—
PACVD DLC, indented	− 350	820	0.4	1120	− 180	0.06	—

Since samples were not scanned cathodically to remove any passive layer before commencing each test and because of their relatively stable and inert nature all of the coatings used were expected to have been fully passive throughout the full range of scanned potentials but this was not so. Notable features which emerged from the cyclic polarization study of coated samples included the somewhat surprising fact that under some conditions all three coatings revealed the presence of an active corrosion range in the initial stages of polarization, and some evidence for tranpassive breakdown at higher potentials (see Fig. 6d). CrN deposited onto glass has been shown to be completely free from active or transpassive behavior and remains passive over a wide range of potentials [17]. Passivation currents were significantly higher for the polished CrN coated samples than for any of the other coatings or condition.

Transpassive breakdown occurred in all samples tested except for the thick (19 μm) TiN coating. Evidence of transpassive breakdown occurred within both the thin TiN coating and DLC coatings despite the expectation that both should have behaved as stable materials.

Table II shows that samples coated with TiN or DLC tended to have higher breakdown potentials and currents than the uncoated cobalt alloy under all conditions but that the breakdown potential was reduced by indenting the surface with hardness indentations. The highest breakdown potentials and passive range ΔE recorded occurred with the TiN coated alloys.

CrN coated alloys gave very similar passive ranges, and breakdown potentials to those found with the uncoated cobalt alloy, especially after being indented with hardness indents to expose the cobalt substrate. Such a result suggested that some chemical similarity existed between CrN and the Cr_2O_3 oxide film normally regarded as being responsible for passivation in Co–Cr–Mo alloys and supported possibilities that the passivation response of the coating was being influenced by the presence of chromium oxides within or on the coating. Significant pitting attack took place at defects contained by the coating when samples were polarized into the transpassive range (see Fig. 8), and were assumed to consist of chromium metal micro metal droplets co-deposited during the evaporative coating process. Sonobe *et al*. [20], also discovered that CrN coatings produced by a multi-stage PVD method showed better corrosion resistance than coatings made by a conventional PVD method and attributed this improvement to a decrease in the number of defects in the coating film.

These droplets could not be positively identified or distinguished as being different in composition to the surrounding CrN coating by energy dispersive analysis or by X-ray mapping but they were shown to be chromium rich and produced a different back scattered imaging response than the CrN, due to their higher

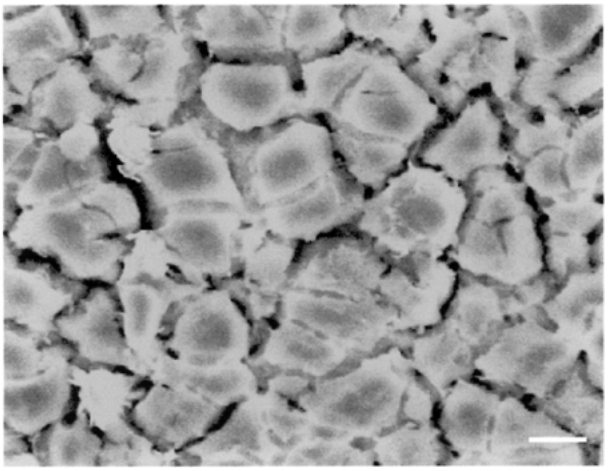

Figure 7 Severe grain boundary attack caused by transpassive breakdown of the cobalt alloy. SEI image. Mag × 800.

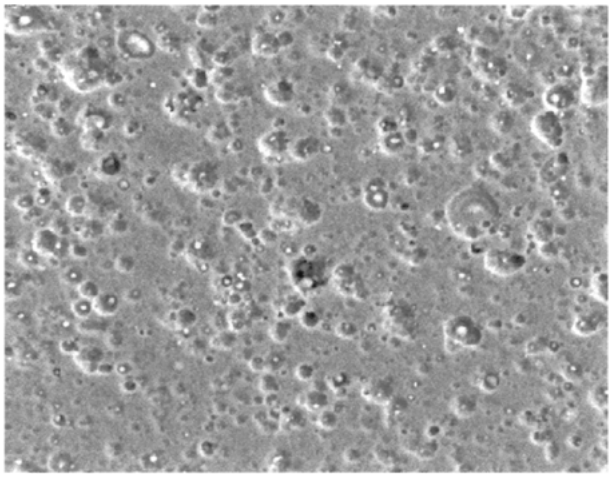

Figure 8 Pitting produced on the surface of a CrN coating after cyclic polarization. Pitting was associated with micro metal droplets of chromium. SEI image. Mag × 800.

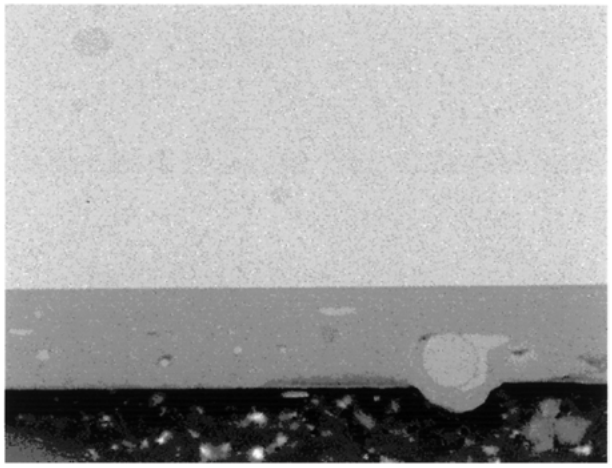

Figure 9 Cross section of chrome metal droplet formed in CrN coating. Note how it protrudes from the surface and the shrinkage cavities formed below the droplet. The chrome metal zone appears to be covered by either an oxidized or nitrided layer. BSE image. Mag × 2500.

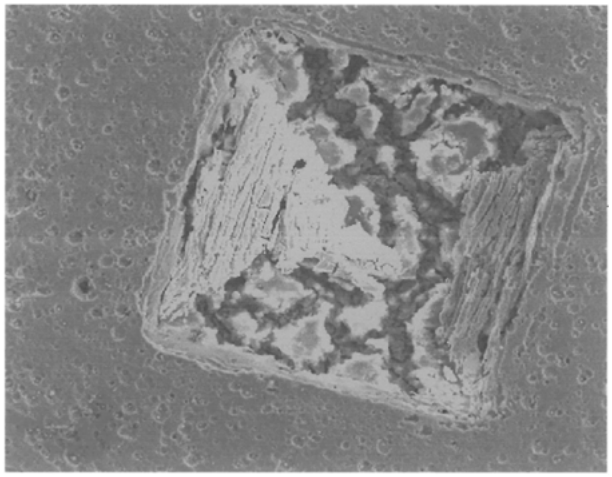

Figure 10 Attack in cobalt alloy substrate exposed by hardness indent made in CrN coating. Note retention of coating integrity around the indent and the presence of general pitting within the CrN coating. SEI image. Mag × 400.

atomic number. The droplets also appeared to be coated by their own film of either chromium nitride or possibly Cr_2O_3 metal oxide films which may have formed spontaneously by exposure to air, or by oxide contamination during PVD coating (see Fig. 9). Anecdotal evidence that the film formed around chromium metal droplets may have contained oxide was seen by its slight differences in atomic number contrast level compared to the CrN coating and by a tendency for droplets to charge up under the electron beam owing to their poor electrical conductivity.

More of these defects were exposed at the coating surface and the nitride/oxide film surrounding them was removed by polishing so that the extent to which pitting attack took place was worse after the CrN coating had been polished; this probably accounted for the unusually high passivation and breakdown currents densities observed with the polished CrN coating (see Table II). No evidence of any corrosive attack of the cobalt alloy substrate due to poor coating adhesion or by penetration of the CrN coating around micro metal droplets was found.

Pitting attack of the cobalt alloy of the same form as that seen in the uncoated alloy, occurred wherever the CrN coating was indented to expose the underlying cobalt substrate. No loss of coating or increase in the extent of corrosive attack to the CrN coating occurred at the edges of the indented region and any corrosion which took place within the exposed cobalt alloy did not spread beyond the confines of the hardness impression (see Fig. 10). No evidence was found to show that the coating had become undermined by corrosive attack at the coating /substrate interface. CrN coatings did not therefore encourage galvanic attack of the substrate by dissimilar metal contact where the underlying cobalt alloy became exposed.

Despite there being some similarities in behavior for both the CrN coated and the uncoated cobalt alloy, however, the overall corrosion resistance and potential metal ion release rate caused by migration through the passive layer was significantly improved by the application of a CrN coating. Firstly, the current densities produced within both the passive and transpassive ranges were significantly lower after CrN coating than in the cobalt alloy substrate. Secondly, the CrN coated surface still remained intact and unlike the uncoated cobalt alloy, was not massively attacked or penetrated after being exposed to transpassive corrosion at highly positive potentials, see Fig. 10. Any corrosion that did occur took place at defects present in the coating surface. Repassivation of the CrN surface during the reverse cathodic scan occurred at almost the same potential as that which produced the original transpassive breakdown and little hysteresis or crossover between the forward and reverse scan took place. CrN coatings could thus be regarded as being resistant to pitting attack.

TiN coatings were expected to behave as extremely stable materials with no signs of either active corrosion or transpassive breakdown over the entire range of potentials used in cyclic polarization, but this was not the case, especially for the thin 8 μm coating. TiN coatings also contained micro metal droplets, which were assumed to be titanium metal, plus numerous small pores. Unlike the CrN, however, microscopic examination revealed no evidence of serious corrosive attack around the micro metal droplets in either the thick or thin TiN coating. Such findings were contrary to expectation given that clear signs of active corrosion and of transpassive breakdown occurred during cyclic polarization with thin TiN coatings. The only possible explanation for this was that corrosion was occurring within the cobalt alloy substrate beneath pores in the TiN coating. Contact between the cobalt alloy and relatively large areas of stable TiN tended to produce a system with a fairly negative rest potential at which the cobalt alloy was polarized to a level below its passivation potential where it became incapable of maintaining its normal passive protection. Potential for localized attack by either active or transpassive corrosion might thus exist where any cobalt substrate was unprotected by its TiN coating both at low and high potentials and rapid attack could arise by virtue of the having a large cathode and small anode area condition. Severe transpassive corrosive attack took place at areas of cobalt alloy exposed by hardness indentation and also at pores in the thinner of the two TiN coatings (see Fig. 11). Large differences between the chemical stability of TiN compared with the cobalt alloy also developed high driving forces for

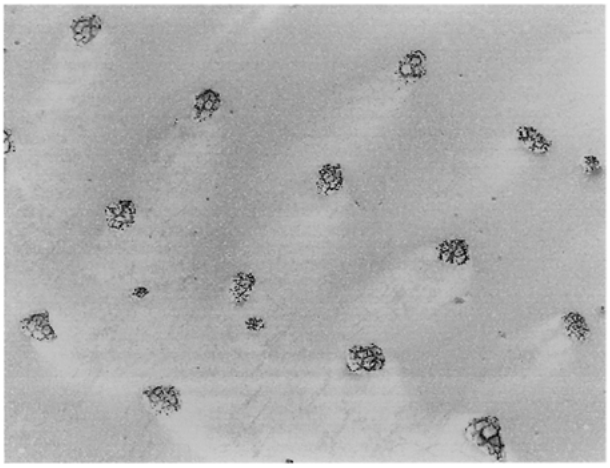

Figure 11a Attack caused by cyclic polarization of an indented TiN coating. Note severe corrosion of the exposed cobalt alloy both at indented sites and at other defects in the TiN coating. SEI image. Mag × 50.

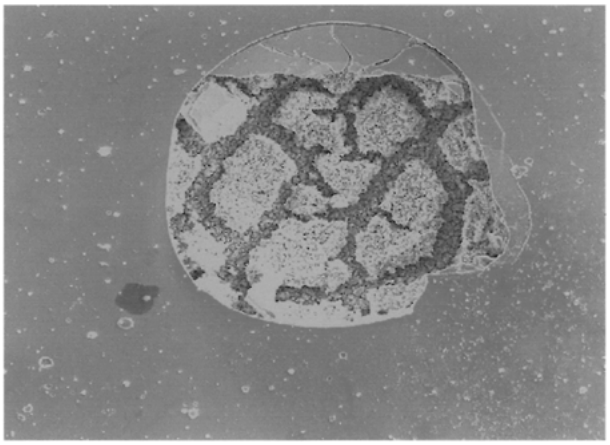

Figure 11b Attack caused by cyclic polarization of a TiN coating. Note severe corrosion of the exposed cobalt alloy at coating defect in the TiN coating. Corrosion of the substrate and loss of coating has spread well beyond the confines of the original defect. SEI image. Mag × 800.

galvanic attack so that severe corrosive attack took place in the cobalt substrate and damage spread sideways to produce deep pits and loss of coating as it became undermined by attack to the substrate (see Fig. 9). Pitting attack of the cobalt through pores in the TiN might also account for the delay in repassivation and consequent hysteresis found under reverse cathodic scanning in the cyclic polarization study of the thinner TiN coated samples (see Fig. 6b). No such problems arose with the thick TiN coating because pores in the surface did not penetrate to reach the underlying cobalt alloy.

DLC coatings showed no visual signs of corrosive attack after cyclic polarization despite the evidence of transpassive breakdown (see Fig. 6d). Severe corrosion took place, however, in areas of cobalt alloy substrate exposed by hardness indentation and attack spread well beyond the confines of the original hardness impression (see Fig. 12). The DLC coating also exhibited higher transpassive breakdown potentials and currents than found for the cobalt alloy substrate but had lower breakdown potentials than found with TiN coating.

DLC is a dense, metastable form of amorphous carbon (a-C) or hydrogenated amorphous carbon (a-C : H) containing significant sp^3 bonding. The sp^3 bonding

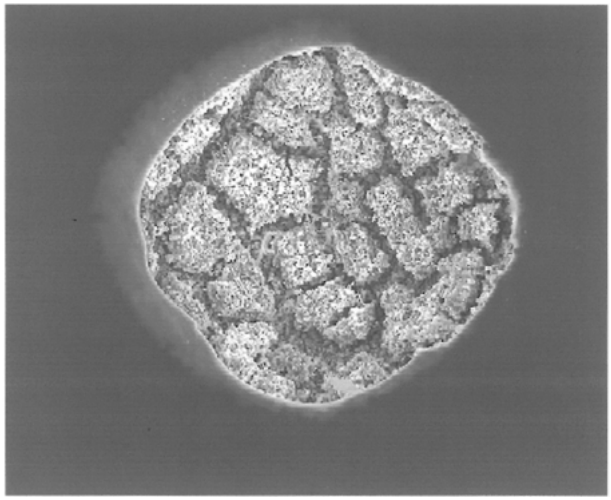

Figure 12 Attack caused by cyclic polarization of an indented DLC coating. Note severe corrosion of the exposed cobalt alloy both at indented sites and at other defects in the TiN coating. Corrosion of the substrate and loss of coating has spread well beyond the confines of the original indent. SEI image. Mag × 400.

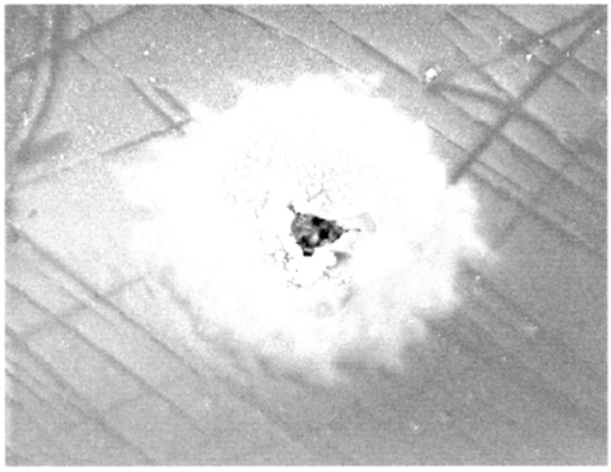

Figure 13 Corrosion of cobalt alloy substrate produced at a pore within the DLC coating. SEI image. Mag × 400.

confers ''diamond-like'' properties such as mechanical hardness, low friction, chemical inertness and high electrical resistance which might be expected to produce high resistance to transpassive breakdown and low corrosion currents. The relatively high current densities recorded suggested that DLC coatings imposed little barrier to the transport of metallic ions or electrons between the metal substrate and corrosive solution. Good electrical conductivity may have arisen from the presence of a conducting graphite phase within the DLC coating structure, but this would be unlikely to create better conductivity than was observed for the uncoated cobalt alloy. Alternatively, relatively high current densities could have arisen because of poor coating adhesion, as previously suggested by Dowling *et al*. [21], or because of the presence of micron sized defects inherited during coating deposition which allowed penetration of the physiological test solution through to the underlying substrate, as suggested by previous work [22, 23]. This later suggestion appears most likely and some evidence of attack at pores was found (see Fig. 13).

Conclusions

1. All three coatings were more resistant to transpassive breakdown and remained passive over a wider range of potential than the uncoated cobalt alloy.

2. Relatively thick CrN coatings were not penetrated by corrosive attack and provided excellent protection to the underlying cobalt alloy. The coating was however susceptible to pitting attack when polarized into the transpassive range. Attack took place at chromium metal micro droplets co-deposited with the CrN coating. Suspicions were aroused that this form of attack might occur during long term exposure at normal rest potential and the evidence suggested that coating passivity could breakdown at only moderately high polarization potentials.

3. TiN coatings were less heavily attacked at micro metal defects present within the coating and gave excellent protection providing they produced complete coverage of the surface. Concerns were raised that some risk of accelerated corrosion of the underlying cobalt alloy might occur if defects, or pores or areas of mechanical damage allow the underlying substrate alloy to become exposed.

4. Although the DLC coatings supposedly have high electrical resistance and chemical inertness, they were the least effective of the three coatings. This was attributed to lack of coating thickness and to its inherent porosity and lack of adhesion.

Acknowledgments

The authors like to thank Ion Bond Ltd (UK) for providing all the coating samples used in this research. This work was financially supported by The Engineering and Physical Sciences Research Council (EPSRC) in Great Britain.

References

1. R. A. COOPER, C. M. MCALLISTER, L. S. BORDEN and T. W. BAUER, *J. Arthroplasty* **18** (1992) 285–290.
2. H. C. AMSTUTZ, P. CAMPBELL, N. KOSSOVSKY and I. C. CLARKE, *Clin. Orthop.* **276** (1992) 7–18.
3. T. P. SCHMALZRIED, E. S. SZUSZCZEWICZ, K. H. AKIZUKI, T. D. PETERSON and H. C. AMSTUTZ, *Clin. Ortho. Rel. Res.* **329** (1996) 48–559.
4. N. A. ATHANASOU, J. QUINN and C. J. K. BULSTRODE, *J. Bone Joint Surg.* **74B** (1992) 57–62.
5. F. W. CHAN, J. DENNIS BOBYN, J. B. MEDLEY, J. J. KRYGIER, S. YUE and M. TANZER, *Clin. Ortho. Rel. Res.* **333** (1996) 96–107.
6. T. P. SCHMALZRIED, P. C. PETERS, B. T. MAURER, C. R. BRAGDON and W. H. HARRIS, *J. Arthroplasty* **11** (1996) 322–331.
7. P. F. DOORS, P. A. CAMPBELL, J. WORRALL, P. D. BENYA, H. A. MCKELLOP and H. C. AMSTUTZ, *J. Biomed. Mat. Res.* **42** (1998) 103–111.
8. J. J. SCHEY, *Clin. Orthop.* **329S** (1996) 115–127.
9. P. DOORN, J. M. MIRRA, P. A. COMPBELL and H. C. AMSTUTZ, *ibid.* **329S** (1996) 187–205.
10. M. K. HARMAN, S. A. BANKS and W. HODGE ANDREW, *J. Arthroplasty* **12** (1997) 938–945.
11. M. SIVAKUMAR and S. RAJESWARI, *Steel Research* **66** (1995) 35–38.
12. D. W. HOWIE, S. D. ROGERS, M. A. MCGEE and D. R. HAYNES, *Clin. Orthop. Rel. Res.* **329S** (1996) S217–S232.
13. R. F. COLEMAN, J. HARRINGTON and J. T. SCALES, *Brt. Med. J.* **1** (1973) 527–529.
14. K. MERRITT and S. A. BROWN, *Techniques Orthop.* **8** (1993) 228–236.
15. J. J. JACOBS, J. BLACK, A. K. SKIPOR and W. P. PAPROSKY, L. M. PATTERSON, J. O. GALANTE, *Trans. Annual Soc. Biomaterials* **1** (1996) 243.
16. B. S. BECKER, PhD thesis, Department of Mechanical and Medical Engineering, University of Bradford, UK (1996).
17. G. BERTRAND, H. MAHDJOUB and C. MEUMIER, *Surface Coat. & Technol.* **126** (2000) 199–209.
18. H. D. STEFFAN, M. MACK, K. MOEHWALD and K. REICHEL, *ibid.* **46** (1991) 65.
19. H. W. WANG, M. M. STACK, S. B. LYON, P. HOVSEPIAN and W. D. MINTZ, *ibid.* **126** (2000) 279.
20. M. SONOBE, K. SHIOZAWA and K. MOTOBAYASHI, *JSME Inter. J.* **40** (1997) 436–444.
21. D. P. DOWLING, P. V. KOLA, K. DONNELLY, T. C. KELLY, K. BRUMITT, L. LLOYD, R. ELOY, M. THERIN and N. WEILL, *Diamond and Related Materials* **6** (1997) 390–393.
22. L. CHANDRA, M. ALLEN, B. BUTTER, N. RUSHTON, A. H. LETTINGTON and T. W. CLYNE, *ibid.* **4** (1995) 852–856.
23. R. S. LILLARD, D. P. BUTT, T. N. TAYLOR, K. C. WALTER and M. NASTASI, *Corrosion Science* **39** (1997) 1605–1624.

Received 8 February
and accepted 3 April 2001